Thermal contact resistance between graphene and silicon dioxide

Z. Chen; W. Jang; W. Bao; C. N. Lau; C. Dames

Check for updates

View Online

Export Citation
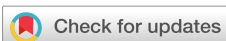
Articles You May Be Interested In

Thermal contact resistance between graphene and silicon dioxide

Z. Chen,[1] W. Jang,[1] W. Bao,[2] C. N. Lau,[2] and C. Dames[1,a)]

[1]*Department of Mechanical Engineering, University of California, Riverside, California 92521, USA*
[2]*Department of Physics and Astronomy, University of California, Riverside, California 92521, USA*

The thermal contact resistance between graphene and silicon dioxide was measured using a differential 3ω method. The sample thicknesses were 1.2 (single-layer graphene), 1.5, 2.8, and 3.0 nm, as determined by atomic force microscopy. All samples exhibited approximately the same temperature trend from 42 to 310 K, with no clear thickness dependence. The contact resistance at room temperature ranges from 5.6×10^{-9} to 1.2×10^{-8} $m^2\,K/W$, which is significantly lower than previous measurements involving related carbon materials. These results underscore graphene's potential for applications in microelectronics and thermal management structures. © *2009 American Institute of Physics*. [doi:10.1063/1.3245315]

Graphene—a single (or a few) layer(s) of graphite, or, equivalently, an unrolled single-wall (or multiwall) carbon nanotube—exhibits many remarkable physical properties that attract both fundamental and applied interest.[1] In particular, although challenges remain in wafer-scale deposition and controlling the electronic bandgap, graphene is widely seen as a strong candidate for postsilicon microelectronics because of its ultrahigh electron mobility[1] and high thermal conductivity.[2,3] To ensure effective heat transfer away from active devices and into heat sink regions, future graphene-based microelectronics, interconnects, and thermal management structures will require good thermal contact between graphene and other materials, especially dielectrics.

The thermal contact resistance is defined as the temperature difference across an interface per unit heat flux, and is the most common quantity used to characterize interfacial heat transfer. Although no direct measurements have been reported to date for the thermal contact resistance between graphene and any other material, the thermal contact resistance of several related carbon materials has been measured by various groups. For example, using a transient thermoreflectance technique, Schmidt *et al.*[4] measured the thermal contact resistance between a highly ordered pyrolytic graphite substrate and an Al thin film to be 2.0×10^{-8} $m^2\,K/W$ at 300 K. Yu *et al.*[5] measured the thermal contact resistance between a 152 nm diameter carbon nanofiber and a Pt substrate; based on the reported contact width (10 nm), and our estimates of the contact length from the published scanning electron microscope images, the equivalent thermal contact resistance of the nanofiber is $4.4-6.7\times10^{-8}$ $m^2\,K/W$ at room temperature. For single-walled carbon nanotubes on SiO_2 substrates, by fitting the measured electrical breakdown voltages to a thermal model, Pop *et al.*[6] extracted a contact resistance equivalent to $1.0-2.1\times10^{-8}$ $m^2\,K/W$ from $500-700\ ^\circ C$.

Here we report measurements of the thermal contact resistance between single- and few-layer graphene and silicon dioxide, using a differential 3ω method[7] over a temperature range from 42 to 310 K. The sample fabrication is summarized in Fig. 1. First, graphene flakes are deposited randomly on an oxidized Si wafer using an exfoliation method.[1,8] Al-

though it would be desirable for the bottom oxide to be thinner in order to minimize the background thermal resistance, we are restricted to use a 300 nm thick layer because of the optical interference method used to identify the thin flakes.[1] Candidate flakes are then located with respect to a grid of alignment marks. Next we anneal the samples with Ar (1.7 l/min) and H_2 (1.9 l/min) at 400 °C for 1 h,[9] followed by electron-beam evaporation of approximately 30 nm of silicon dioxide. Then electron-beam lithography is used to pattern evaporated Cr/Au electrodes (thickness 5 nm/175–345 nm) by a lift-off process. Finally, we use an argon ion beam (inductively coupled plasma at 450 W, with 50 W of rf power) to mill the top surface of the sample to an etch depth slightly greater than the original thickness of the top oxide. In this way the graphene flake is trimmed to match the width of the metal heater line, which ensures one dimensional heat flow through the graphene flake, simplifying subsequent thermal analysis. To facilitate the differential 3ω measurements, on
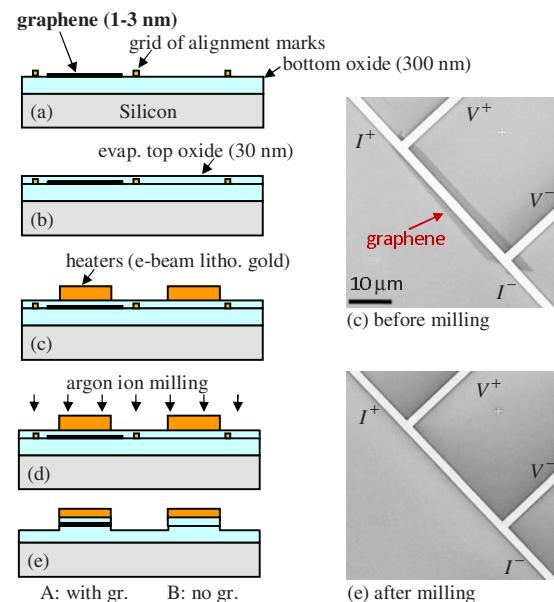

FIG. 1. (Color online) Sample microfabrication. (a) Deposit and locate graphene flakes. (b) Cleaning anneal, then evaporate top oxide. (c) Pattern the heaters. [(d) and (e)] Ion mill the top surface using an Ar beam, to trim the flake and simplify the thermal analysis.

25 January 2026 10:07:22

every sample we fabricate two heaters in close proximity with identical heater patterns and etch depths: the primary pattern ("A") which includes the graphene flake between the oxide layers, and a control pattern ("B") with top and bottom oxide layers but no graphene [Fig. 1(e)].

The experiments are conducted at temperatures from 42–310 K in a liquid helium cryostat evacuated to $\sim 10^{-6}$ Torr. Although differential 3ω methods most commonly use a single value of the electrical current and evaluate the difference between two frequency sweeps,[7] we have found somewhat improved uncertainty by fixing the frequency (at 1000 Hz) and evaluating the difference between two current sweeps. In this scheme we check the linearity of the curve of heater temperature rise versus power, to verify that the current and voltage are free of offset errors and nonthermal harmonics. We confirmed that the final results are independent of the frequency chosen for the current sweep. For example, contact resistance measurements taken at 10, 500, 1000, and 10 000 Hz agree to within $\pm 3.8\%$ at 310 K and $\pm 2.2\%$ at 80 K [95% confidence interval (CI)].

For each sample we determine the ac thermal impedances of the primary (Z_A) and control (Z_B) patterns from the slope of the heater temperature rise versus power.[10] Subtracting the two impedances gives the differential thermal resistance due to the encased graphene: $Z_A - Z_B = (R_{g \leftrightarrow \text{top ox}} + R_{g \leftrightarrow \text{bot. ox}}) - R_{\text{top ox} \leftrightarrow \text{bot. ox}}$. We assume the thermal contact resistances from graphene to top and bottom oxides are identical ($R_{g \leftrightarrow \text{top ox}} = R_{g \leftrightarrow \text{bot. ox}} = R_{g \leftrightarrow \text{ox}}$), and neglect the contact resistance between the top and bottom oxide layers in the control pattern ($R_{\text{top ox} \leftrightarrow \text{bot. ox}} \ll 2R_{g \leftrightarrow \text{ox}}$). Thus, we calculate $R_{g \leftrightarrow \text{ox}} = \frac{1}{2}(Z_A - Z_B)$.

The largest contribution to the overall uncertainty in $R_{g \leftrightarrow \text{ox}}$ is the uncertainty in the temperature response of the electrical resistance of the heater, dR_e/dT. As shown in Fig. 2(a), a simple linear fit $R_e = a_0 + a_1 T$ is clearly inadequate to describe the calibration curve $R_e(T)$ over the large temperature ranges of interest. Therefore, for every heater pattern we fit the measured $R_e(T)$ with a Bloch–Grüneisen (BG) formula $R_{e,\text{BG}}(T)$ containing three adjustable parameters,[11] which as shown in Fig. 2 is a much better description of the experimental $R_e(T)$. As expected the residuals of this improved fit reveal small but clear deviations from the simple BG theory [Fig. 2(b)].[11] We capture these deviations empirically using a low-order polynomial in $\ln(T)$,

$$R_e(T) \approx R_{e,\text{BG}}(T) + \sum_{n=1}^{N} c_n [\ln(T)]^n, \quad (1)$$

where the results become approximately independent of N for $3 \leq N \leq 5$. Finally, we differentiate Eq. (1) analytically to obtain the required dR_e/dT. [Our final results are taken as the average of the values obtained from the third, fourth, and fifth order versions of Eq. (1)] We analyze the uncertainty propagation using the Monte Carlo method described in Ref. 12.

The measured thermal contact resistances between graphene and SiO$_2$ are shown in Fig. 3 for four samples with different thicknesses (1.2, 1.5, 2.8, and 3.0 nm) as determined by atomic force microscopy (AFM). Based on these AFM measurements[13,14] and our experience with the interference colors under an optical microscope,[2,8] we believe that the 1.2 and 1.5 nm samples are single layer and bilayer
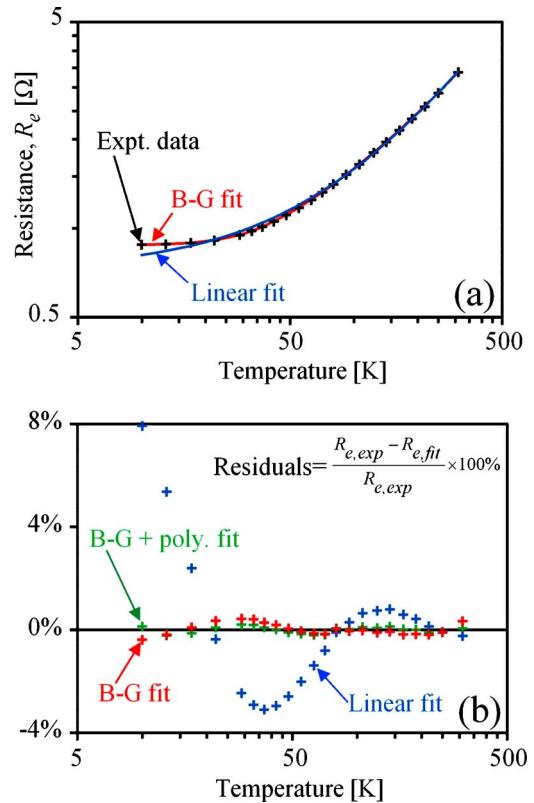

FIG. 2. (Color online) Fitting the electrical resistance of a typical heater. (a) Comparison between the experimental data (points) and the fits using a linear (blue line) or BG formula (red line). On these logarithmic axes the linear fit appears curved. (b) Residuals for the linear fit (blue), BG fit (red), and BG+empirical polynomial fit [green; see Eq. (1)].

graphene, respectively. As shown in Fig. 3, the typical uncertainty in the contact resistance ranges from approximately $\pm 7\%$ at 310 K to $\pm 28\%$ at 42 K (95% CI). At room temperature the contact resistance is found to range from 5.6 $\times 10^{-9}$ to 1.2×10^{-8} m^2 K/W, which is relatively low compared to typical values reported for various other material pairings,[15] and in particular is lower than previous measurements of the contact resistance of carbon materials to various substrates.[4–6,16]
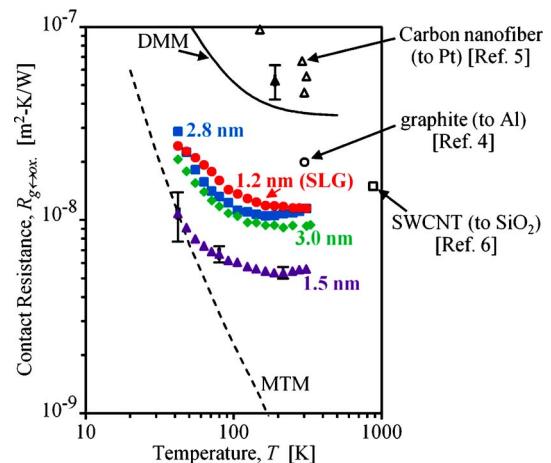

FIG. 3. (Color online) Experimental measurements of the thermal contact resistance between silicon dioxide and graphene, for four samples of different thicknesses as determined by AFM (filled points, in color). Also included for comparison are the contact resistances of several related carbon materials from the literature (open points), and theoretical curves for a DMM and a MTM (lines).

Although the measurements in Fig. 3 do not exhibit any clear dependence on the sample thickness, all four samples follow roughly the same temperature trend. Around room temperature, the contact resistance is relatively independent of temperature, although two of the samples show a slight minimum in $R_{g\leftrightarrow ox}(T)$ around 200 K. Below about 100 K, all four samples show a marked increase in contact resistance, transitioning to a power law that can be approximated as $R_{g\leftrightarrow ox} \propto T^{-1}$.

Modeling the thermal contact between graphene and silicon dioxide is challenging due to the amorphous nature of the SiO_2 and the highly anisotropic properties of the graphene. Here we briefly consider two simple models as shown in Fig. 3. First, a lower bound on the thermal contact resistance is the "maximum transmission model" (MTM),[17] a generalization of the "phonon radiation limit."[18] The phonon internal energies were determined from experimental values of the heat capacity.[19] The characteristic velocities were taken as 4487 and 2157 m/s for oxide (isotropic) and graphene (*c*-axis),[19] respectively, determined from a weighted average of the transverse and longitudinal acoustic sound speeds. Using the *c*-axis velocities for graphene is appropriate for describing the upper limit of heat transfer in this direction. The second model considered in Fig. 3 is the elastic diffuse mismatch model (DMM) described by Duda *et al.*[20] for thermal contact between isotropic and anisotropic materials.[21] As shown by the dashed (MTM) and solid (DMM) lines in Fig. 3, both models capture certain features in the measurements, but with significant weaknesses. The MTM indeed serves as a lower bound and appears promising below about 60 K, but it greatly underpredicts the true contact resistance at higher temperatures. The DMM qualitatively captures most of the temperature trend, but the DMM values are too large by a factor of approximately 6 at all temperatures, which may indicate that inelastic phonon scattering (neglected in this implementation[20]) is a significant channel for heat flow.

In summary, we have measured the thermal contact resistance between graphene and silicon dioxide from 42 to 310 K, and found resistance values significantly lower than previous measurements involving related carbon systems.[4–6] These measurements should prove helpful for interpreting recent experiments involving heat transfer and energy dissipation in graphene,[2,3,22,23] and are an encouraging development for possible future applications of graphene in microelectronics, interconnects, and thermal management structures.

[1] K. Geim and K. S. Novoselov, Nature Mater. **6**, 183 (2007).
[2] A. A. Balandin, S. Ghosh, W. Bao, I. Calizo, D. Teweldebrhan, F. Miao, and C. N. Lau, Nano Lett. **8**, 902 (2008).
[3] W. Jang, Z. Chen, W. Bao, C. N. Lau, and C. Dames (unpublished).
[4] A. J. Schmidt, X. Chen, and G. Chen, Rev. Sci. Instrum. **79**, 114902 (2008).
[5] C. Yu, S. Saha, J. Zhou, L. Shi, A. M. Cassell, B. A. Cruden, Q. Ngo, and J. Li, ASME J. Heat Transfer **128**, 234 (2006).
[6] E. Pop, D. A. Mann, K. E. Goodson, and H. Dai, J. Appl. Phys. **101**, 093710 (2007).
[7] T. Borca-Tasciuc, A. R. Kumar, and G. Chen, Rev. Sci. Instrum. **72**, 2139 (2001).
[8] F. Miao, S. Wijeratne, Y. Zhang, U. C. Coskun, W. Bao, and C. N. Lau, Science **317**, 1530 (2007).
[9] M. Ishigami, J. H. Chen, W. G. Cullen, M. S. Fuhrer, and E. D. Williams, Nano Lett. **7**, 1643 (2007).
[10] C. Dames and G. Chen, Rev. Sci. Instrum. **76**, 124902 (2005).
[11] J. M. Ziman, *Electrons and Phonons* (Oxford University Press, New York, 1960).
[12] W. H. Press, S. A. Teukolsky, W. T. Vetterling, and B. P. Flannery, *Numerical Recipes*, 3rd ed. (Cambridge University Press, New York, 2007) p. 807.
[13] Y.-M. Lin and P. Avouris, Nano Lett. **8**, 2119 (2008).
[14] X. Li, X. Wang, L. Zhang, S. Lee, and H. Dai, Science **319**, 1229 (2008).
[15] H.-K. Lyeo and D. G. Cahill, Phys. Rev. B **73**, 144301 (2006).
[16] Although Refs. 4 and 6 were measured under atmospheric conditions the errors due to convection losses are expected to be negligible.
[17] C. Dames and G. Chen, J. Appl. Phys. **95**, 682 (2004).
[18] N. S. Snyder, Cryogenics **10**, 89 (1970).
[19] R. Nicklow, N. Wakabayashi, and H. G. Smith, Phys. Rev. B **5**, 4951 (1972).
[20] J. C. Duda, J. L. Smoyer, P. M. Norris, and P. E. Hopkins, Appl. Phys. Lett. **95**, 031912 (2009).
[21] R. Prasher, Phys. Rev. B **77**, 075424 (2008).
[22] M. Freitag, M. Steiner, Y. Martin, V. Perebeinos, Z. Chen, J. C. Tsang, and P. Avouris, Nano Lett. **9**, 1883 (2009).
[23] R. Murali, Y. Yang, K. Brenner, T. Beck, and J. D. Meindl, Appl. Phys. Lett. **94**, 243114 (2009).